AUBE '01

12TH INTERNATIONAL CONFERENCE ON AUTOMATIC FIRE DETECTION

March 25 - 28, 2001
National Institute Of Standards and Technology
Gaithersburg, Maryland U.S.A.

PROCEEDINGS

Editors: Kellie Beall, William Grosshandler and Heinz Luck

NIST
National Institute of Standards and Technology
Technology Administration, U.S. Department of Commerce

N. Miyamoto, T. Someya, and T. Omori
Energy & Environmental Technology Laboratory, Tokyo Gas Co., Ltd., Minato-ku, Tokyo, Japan

Field Modeling Of An Initial Stage Of Fire In A Compartment -Comparison with a Fire Experiment Measured in an Enclosure

1. Introduction

Wider installation of the fire detector is effective in preventing disastrous fire. Given a broad variety of fire, effects of the fire and situation of a fire-containing room on fire detection should be well understood, thereby making more effective implementation of fire detectors possible.

The present study focuses on an early stage fire, during which an initiated fire in the compartment develops to trigger a fire detector installed, to elucidate fire phenomena and predict accurately heat transfer and diffusion of combustion-generated intermittent chemical species. To this end, simulation of compartment fire is performed using the field model approach. Existing work of field model fire simulation has largely simplified complex fire phenomena involving turbulent buoyant flow, unsteadiness, chemical reaction of combustion, thermal radiation between the high temperature flame and solid walls, among others.

It has been recognized, however, that in the initial stage of fire, combustion, fluid flow, unsteady heat conduction of building walls, radiative heat transfer from the fire source to the combustion gas as well as walls, and convective heat transfer all play major roles. Hence, putting early stage-fire simulation into practice need to integrate these important factors without oversimplification and by balancing with constraints from computational resources and allowable time frames.

2. Brief Description of Fire Experiment

According to the European standard of fire alarm test method [1], response time of the ceiling-mounted fire sensor provided is measured when a prescribed amount of

combustible is ignited in an enclosure for fire experiment (Fig. 1). Six different types of fuel, designated TF1 for wood through TF6 for ethanol, are prepared to represent fire ranging from flaming fire to smoldering. Here, experimental data for TF6 collected in a thermal detection test [2] are employed for validation of numerical simulation results.

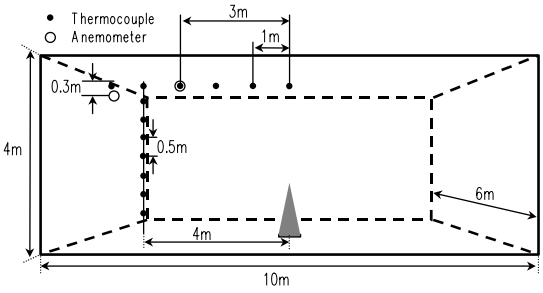

Fig. 1 Schematic diagram of Test Fire Cell

Table 1 Properties of walls, ceiling and floor

Surface	Material	Thermal conductivity	Thickness	Density
		W/mK	m	kg/m^3
Walls	Concrete(Light)	0.523	0.1	1,350
Ceiling	Flexible board	0.616	0.1	723
Floor	Concrete	1.63	0.1	2,250

Table 2 Experiment condition

Comartment size	10 m□ ~6 m□ ~4 m (H)
Fuel	Ethanol2500cc
Pan size	0.435 m □ ~0.435 m
Heat release rate	100 kW
Thermocouple placement (K type)	
Ceiling temperature (horizontal array)	5cm under ceiling
	1m horizontal intervals from fire
Vertical temperature (vertical array)	4m away horizontally from fire
	0.5m vertical intervals from ceiling
Anemometer placement (Ultrasonic anemometer)	
Velocity near by ceiling	5cm under ceiling
	3m away horizontally from fire
Velocity near by wall	30cm under ceiling
	5cm from wall

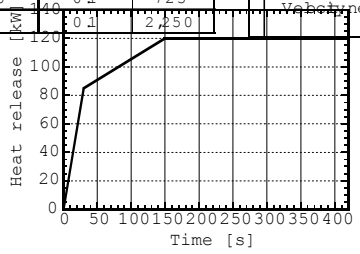

Fig. 2 Heat release rate history

For representative flame combustion, 2500 cc of TF6 ethanol fuel fills a square pan having side length of 43.5 cm placed on a scale that is centrally located on the floor. The thermal properties of the wall material used in the test compartment are summarized in Table 1. When the fuel is spark ignited, ethanol temperature rises by receiving heat from the flame by convection and radiation as well as conduction through the pan walls. After the liquid temperature reaches the boiling temperature of ethanol (351.7 K), all the heat input is consumed by evaporation and both the temperature and the evaporation rate stay constant thereafter. The measured combustion rate using the scale is converted to the heat generation rate and is presented in Fig. 2.

3. Numerical Simulation

3-1. Combustion model

The heat generation rate increases with time in the initial stage of fire studied here and, therefore, its effects should be properly accounted for when one wishes to gain accurate prediction of temperature rise inside the room. To this end, the eddy break up model of Magnussen for combustion [3] is employed. The computations are made under the condition that vaporized ethanol with minimum heat generation of 26.8 MJ/kg, latent heat of evaporation of 0.85 MJ/kg, and specific heat of liquid of 2.42 kJ/kg·K, flows uniformly from the fuel pan into the room. The incoming velocity is set equal to the experimental data.

3-2. Radiative Heat Transfer

Ethanol undergoing liquid surface combustion generates glowing flame with a measured absorption coefficient of approximately 0.4 to 0.5 m^{-1} [4]. The present investigation adapts 0.5 m^{-1} for the absorption coefficient that is specified in a rectangular parallelpiped region above the fuel pan.

At 7 minutes after ignition, the concentration of carbon dioxide (CO_2) below the ceiling is measured to be about 1.1 % in standard wet gas condition, while that of water vapor (H_2O) is 1.6 %. Using the measured gas temperature of 90 °C and by assuming 2.7 m as the thickness of gas layer, the mean light path is estimated to be 2.8 m. The absorption coefficient calculated from the emissivity of gas using the Hottel chart is 0.08 m^{-1}.

As to the absorption coefficient underneath the ceiling, two values – 0.1 m^{-1} (Case 1) accounting for a small amount of soot, and 0.2 m^{-1} (Case 2) – are specified to assess effects of soot radiation.

3-3. Incoming Turbulent Energy of the Fuel

Application of the standard k-ε model to an intensely buoyant thermal plume flow that may arise in fire situations has been found to give overprediction in the axial temperature of plume. This has been attributed to the suppressed momentum and heat diffusion near the fire source [5]. Yoshie et al. [6] obtained closer agreement with the experimental correlation of Yokoi [7] when larger incoming kinetic energy of

turbulence k was specified at the height seven times the radius of the fire source, which leac ects of this practice are examined in the present study by of k for the following three cases: 0.0001 (Case 3, base 0.05 m^2/s^2 (Case 5).

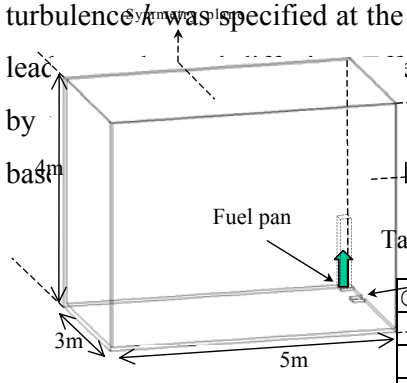

Fig. 3 Simulation model

Table 3 simulation cases

Case	K pr.	k inlet
1	0.1	0.0001
2	0.2	↑
3	0.1	0.02
4	↑	0.05

Table 4 Simulation condition

Time [s]	0 1	3	10	20	40	420
ƒ t [s]	0.1	0.2	0.5	1.0	2.0	5.0
Heat Transfer to Walls	Wall Function (Log law)					
Absorption coefficient [m^{-1}]	Flame	0.5				
	Gas layer	0.1				

3-4. Numerical Method

S age C -ε
r mpress at
t ve hea ed
b ll func re
c e met ty
c e time as
e set sm es

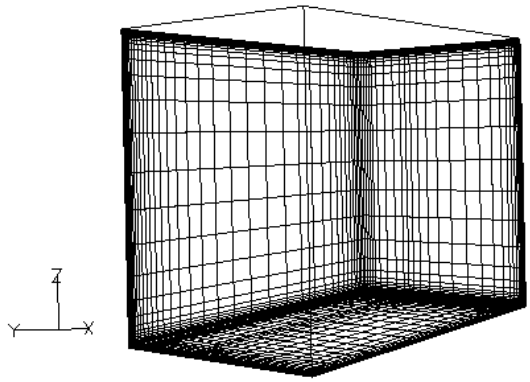

(a) CFD

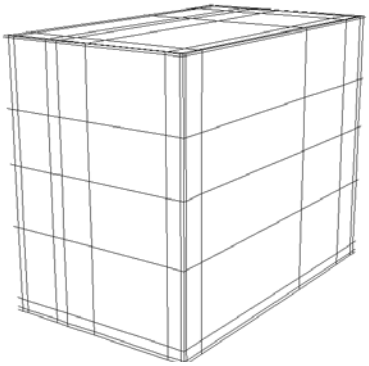

(b)Radiation

Fig. 4 Numerical grids

in the room temper the geometrical symmetry having t ocated in the room, the computation is carried out for a quarter domain only. The incoming flow boundary condition is set at the fuel pan and the drain is treated as a pressure boundary. The simulation model is depicted in Fig. 3. The mesh systems displayed in Fig. 4 have 36,176 grid points consisting of 38 (x) × 28 (y) × 34 (z) divisions for the CFD mesh and 38 × 28 × 34 nodes for radiation calculations. The first CFD grid near the ceiling is located 0.5 cm below the wall. All the computations are run using a SGI Origin 2000 with a single CPU, which consumes about 25 hours per case.

4. Results and Discussion

4-1. Comparison of the Simulated Cases

Figure 5 shows the time history of combustion gas temperature at the point 5 cm underneath the ceiling and 4 m horizontally separated from the fire source. It is seen that the result of Case 1 almost overpredicts the experimental data. On the other hand, in Case 2 for which the absorption coefficient is 0.2 m^{-1}, the computed temperatures increasingly underestimate the measured values with time, indicating the excessively large absorption coefficient. The predicted result of Case 3 with the larger turbulence energy is overall in good agreement with the experiment, except for the temperature overshoot up to 10 °C during t = 100 and 300 seconds. Further increasing turbulence energy (Case 4) leads to much higher temperature with degraded convergence properties stemming from somewhat unstable computation. Based on these observations, the computational results of Case 3 that achieve the best agreement with the measured data are considered for further discussion.

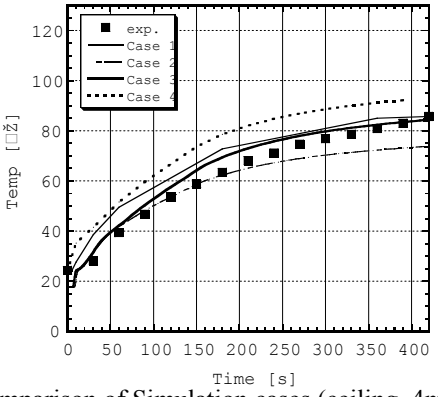

Fig. 5 Comparison of Simulation cases (ceiling, 4m from fire)

4-2. Variation of Vertical Distribution of Air Temperature with Time

The vertical temperature distributions of air at 1, 3, 6, and 7 minutes after ignition at the horizontal location 4 m away from the fire source are represented in Fig. 6. The numerical predictions are seen to be globally in good agreement, although the temperature below the ceiling at 3 minutes is overpredicted by roughly 7 °C and the mid-height temperature undershoots by almost 8 °C at 7 minutes.

4-3. Time Variation of the Near-Ceiling Temperature Distribution of Combustion Gas

In Fig. 7, the horizontal temperature distribution at the monitoring point 5 cm below

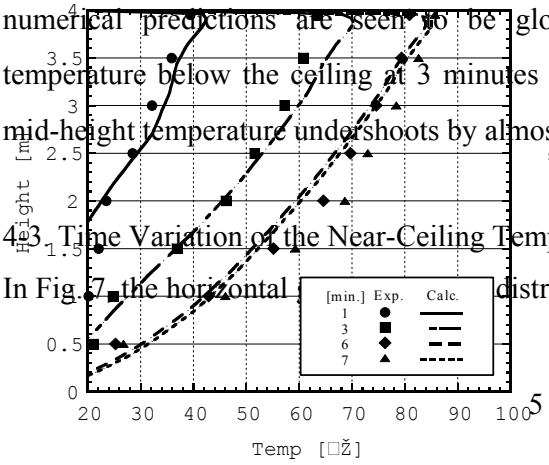

Fig. 6 Transition of vertical temperature distribution (4m from fire)

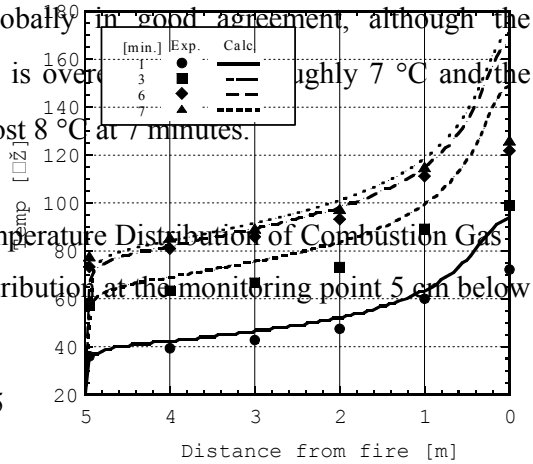

Fig. 7 Transition of horizontal temperature distribution near ceiling

the ceiling from the fire source toward the wall is shown. Except for the computed higher temperature seen right above the fire, the numerical prediction agrees well with the measured results beyond the location 1 m away from the fire.

The European Standard EN54 [1] imposes that the fire detector be positioned on the ceiling and 3 m horizontally away from the location of test fire. The computed temperature will trigger properly a detector with a given temperature sensitivity.

4-4. Flow Velocity

Table 5 provides the measured and computed velocities at 7 minutes after ignition at the location below the ceiling and 3 m separated horizontally from the fire source, and the near wall (distance 5 cm apart) location 30 cm away from the ceiling. The simulation is seen to slightly attain the higher flow speed in both positions. However, in the actual experimental situations in which there are instrumentation and other protrusions on the ceiling area, the flow speed may have been reduced compared to the unobstructed ceiling condition and, in turn, the two sets of data should come closer to be in good agreement.

4-5. Time Elapse to Fire Detector Activation Temperature

The fire detector is designed to activate when the combustion gas temperature at its mounted location reaches 65 °C. Figure 8 depicts the time elapsed from ignition for

Table 5 Velocity comparison at time=390 s

Location	Exp.	Calc.
Ceiling	0.59	0.61
Wall	0.28	0.37

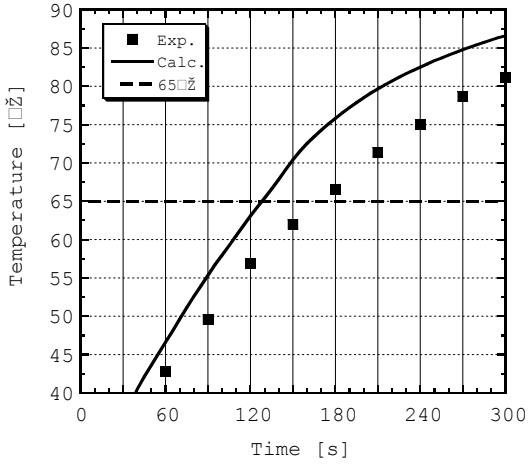

Fig. 8 Comparison of alarm time

triggering the alarm. Note the enlarged scale of temperature centered on 65 °C. The activation time in the experiment is roughly 170 seconds, while in the simulation it is about 40 seconds shorter to have 130 seconds. The difference may stem from the manner the combustion rate is approximated: in the simulation it varies linearly with time, as shown in Fig. 2. More realistic fuel consumption pattern should be utilized for achieving better agreement.

4-6. Variation of Indoor Air Temperature

Changes in the air temperature in the symmetry plane (corresponding to the central vertical plane of the room) together with a plane 5 cm below the ceiling are displayed in Fig. 9. The temperature range exceeding 100 °C is colored in red. After the thermal plume rising from the fire source impinges on the ceiling, it spreads over the ceiling wall in a concentric fashion. Upon hitting the vertical walls, the flow turns downward

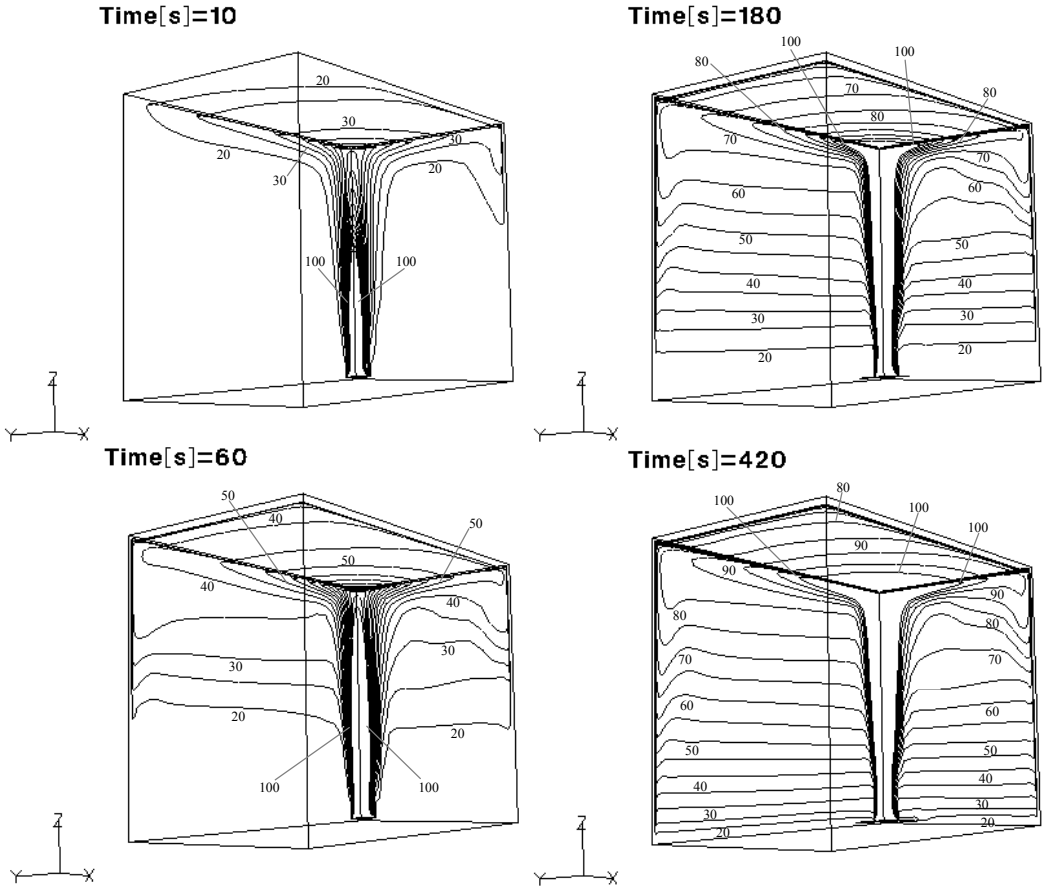

Fig. 9 Transient temperature distributions

until it loses momentum and reverses its direction upward due to the buoyancy force. The nearer the ceiling jet is from the fire source, the larger the momentum contained therein. This manifests into the descending combustion gas that penetrates farther down near the fire source (toward the right of the figure). This demonstrates the course of developing thermal stratification properly captured in the present simulation results.

5. Conclusion

The early stage-fire experimental situation using ethanol fuel (TF6) that conforms to the EN 54 semi-enclosure is simulated numerically by way of the field model approach. The following conclusion is drawn from the results obtained:

1. In the stagnation region where impingement of the thermal plume on the ceiling takes place, the predicted temperatures are significantly higher compared with the measurement data. However, excellent agreement is achieved in the ceiling jet region that is located about 1 m away from the stagnation point.
2. For the numerical simulation of the TF6 fire experiment, the absorptivity of combustion gas layer for thermal radiation is roughly 0.1 m^{-1} that is given by the Hottel chart.
3. With the eddy break up model used for modeling combustion, higher turbulence energy should be assigned as the boundary condition for the incoming fuel. For TF6, good agreement with the experimental result in the ceiling jet region is found by setting $k = 0.02$ m^2/s^2.
4. The present numerical simulation captures successfully a series of phenomena characteristic of the early-stage compartment fire: When the ascending thermal plume from the fire source impinges on the ceiling, it transforms to the ceiling jet that spreads concentrically. The ceiling jet, after it shortly heads downward upon hitting the vertical walls and then loses momentum, rises due to the buoyancy effects. These lead to the well-developed thermal stratification as time elapses.

References

[1] British Standard Institution, Components of automatic fire detection systems: Part 9. methods of test of sensitivity to fire. EN 54 1984.

[2] Doi, M., Manmoto, A. and Yamauchi, Y. Prediction of response time of the thermal sensor using the RTI-C model. Proc. Fire Society of Japan 1999; 50-53 (in Japanese).

[3] Magnussen, B. F. and Hjertager, B. H. On mathematical modeling of turbulent combustion with special emphasis on soot formation and combustion, 16th Symp. (Int.) on Combust. 1976; 719-729.

[4] Tanaka, T. Introduction to Building Fire Safety Engineering 1993; 138-141 (in Japanese).

[5] Nam, S. and Bill, R. G. Jr. Numerical simulation of thermal plumes. Fire Safety Journal 1993; 21: 231-256.

[6] Yoshie, R. CFD Analysis of Fire Plumes (2nd Report). Proc. Arch. Inst. Japan 1998; 147-148 (in Japanese).

[7] Yokoi, S. Study on the prevention of fire-spread caused by hot upward current. Report of the Building Research Institute 1960; No. 34.

[8] CFX Release 4.2 User Guide. 1994; AEA Hyprotech K.K.

[9] Omori, T., Yamaguchi, S. and Taniguchi, H. Accurate Monte Carlo simulation of radiative heat transfer with unstructured grid systems. 11th Int. Symp. on Transport Phenomena 1998; 567-573.